The Physics of T-S waves of Transition to Turbulence (22/10/17: copy at Lerners LLD)
"*The duomo-bell strikes ten....some gaslights tremble along streets and squares*": Aurora Leigh, E.B. Browning,1857

Key words
arteriographic standing waves, candy cane, columnar eddies, counter-rotating vortices, dolphin hydrodynamics, laminar interlocking, rifled rotation, shear waves, simple harmonic sound, SPIV, spiral waves, streaming flows, vibrations and waves

Introduction
The Tollmien-Schlichting (T-S) waves of transition are really composed of three different, but intimately inter-related wave forms. Understanding the factors creating these waves should contribute to the resolution of the problem of the physics responsible for transition to turbulence, a mystery that Schlichting suggested might never be explained [1].

Simple harmonic sound triggers turbulence
Elizabeth Barrett Browning was fascinated by rhythmic sounds [2]. In 1857, in the public readings and discussions of her poem, Aurora Leigh, she shared with the philosophers of her day (audiences composed of academics in the Arts and Sciences) her observation that musical simple harmonic (SH) sound (the peeling of a particular church bell) could suddenly trigger the phenomenon of turbulent flow in a series of gaslight flames "along streets and squares": the smooth steady laminar flow of the gaslights suddenly flickered in unison as a particular church bell tolled [3].

Shortly thereafter, perhaps as a result of Browning's observation in her acclaimed epic poem, Dr. John Leconte noticed at an orchestral performance in 1859, that a sconce gaslight dropped in height, flickered and became noisy as certain notes of a cello triggered turbulence, leading him to perform experiments proving that specific SH sound could precipitate turbulence in laminar jets at lower flow rates, when the flow rate was in the dynamic "sound sensitive" range of transition [4].

In 1867, Sir John Tyndall demonstrated that SH sound, especially when directed transversely to the flow, precipitated turbulence when laminar flow was in the sound sensitive range, concluding that the waveforms of specific SH sound were similar to the waves generated by fluid friction (viscosity) along the wall (boundary) of the tube, amplifying them and triggering turbulence as did a rise in flow rate, believing that this explained turbulence [5].

Candy cane rifling of a cylinder's turbulent flow column
In the Reynolds era, a change in appearance of a cylinder's efflux jet indicated when laminar flow became turbulent: the smooth, shiny surface of the exit jet suddenly changed to a frosted glass appearance. In 1973, freeze-frame photographs of efflux jets from small calibre cylinders revealed that, rather than exhibiting a frosted glass and chaotic flow pattern, the turbulent exit jet displayed a distinctive organized flow pattern – spiral waves with a shiny surface pattern suggesting that the fluid column had acquired rifling as turbulence onset [6].

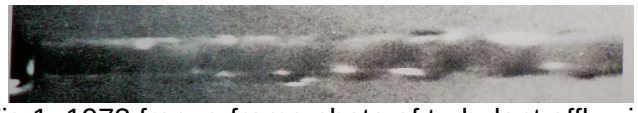
Fig.1: 1973 freeze-frame photo of turbulent efflux jet

1867 experiments with flat flames might point to the cause of the rifled rotation that accompanies the onset of turbulence in cylinders: Tyndall showed that certain specific SH

transverse sound frequencies would not only trigger turbulence, but the flame simultaneously rotated 90 degrees, maintaining the rotation for the duration of the SH sound. Constantly resonating echoing transverse SH sound might have caused the steady axial rotation (rifling) of the turbulent column [7].

Tyndall's horizontal cylinder water flow studies revealed another phenomenon. When the flow rate was in the sound sensitive range, a particular SH sound caused, not only the sudden onset of turbulence but, simultaneously, the efflux jet would divide into 2, 3 or more equal jets, with his illustrations suggesting rifled axial rotation in the efflux jet and in its divisions. It is logical to consider that the physics causing the steady rotation might be related to the physics of transverse SH sound causing the rotation of a flat flame as it triggered turbulence. What is more important is that the 2, 3 or more similar jet divisions are probably the same 2, 3 or more transverse flow divisions found in equal sectors of turbulent cylinder flow columns, in 2004 on SPIV (stereoscopic particle image velocimetry) computerized transverse cylinder flow studies at Delft [8].

Furthermore, the diagonal orientation of longitudinal flows shown repeatedly in SPIV studies of turbulent flow in cylinders is supportive evidence of rifling. The rifled appearance is particularly evident in figures a, b and c, under Mullin's heading "Oblique push-pull disturbance, side view," at Re = 3000 [9], as presented at the 4th Brooke Benjamin Lecture (2010).

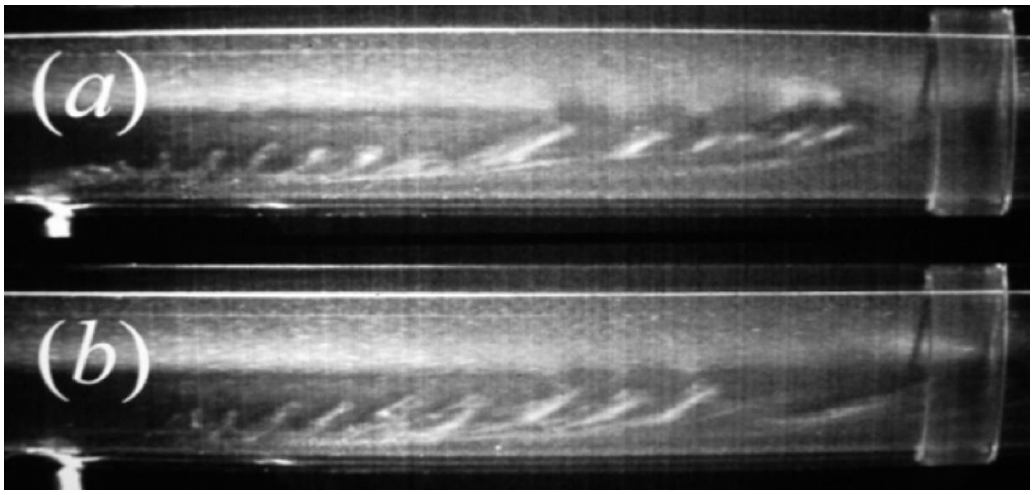

Figure 2: Re = 3000, side view (Mullin et al 2010)

The spiral waves in the computerized images duplicate photographs of the efflux jets from small diameter cylinders (Hamilton 1980 and 2011).

Figure 3: rifled spiraling of turbulent efflux (1973)

If one now adds SPIV coloring to figure 3:

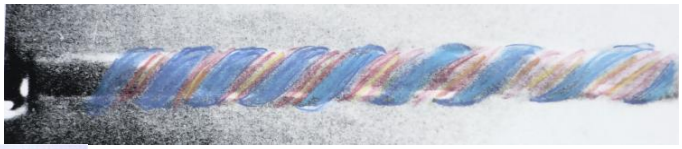

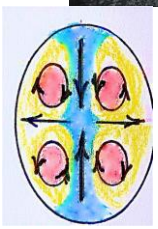

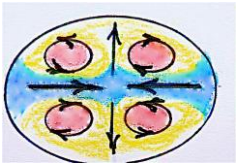

Fig. 4: red = low pressure spiral vortices blue = wider high pressure transverse flows

In 1930, Nikuradse described flow patterns in turbulence in tubes with geometric cross sections. Triangular tubes displayed a signature transverse flow pattern – a streaming centripetal flow from each mid-wall, flanked by a pair of entrained counter-rotating vortices. In a tube with an equilateral triangular cross section, the centripetal flows collide in the tube centre, recirculate towards the corners and then return to the flow origins in the mid-wall boundary layer. Nikuradse believed the faster flows towards the corners were the primary flows, but these are only re-circulations that are accelerated by the converging sides of the triangular tubes.

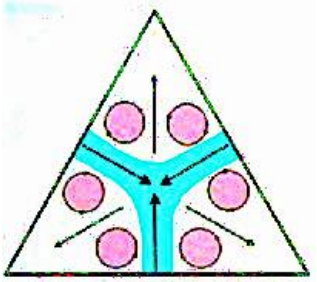

Figure 5: Nikuradse 1930

Two inter-related factors prevented Nikuradse from finding similar flow divisions in cylinders:

1. Rifled spinning occurs in a cylinder's flow column as turbulence onsets.
2. He was limited by 1930 technology.

Nikuradse's cross-sectional vortices in triangular (and other multi-sided geometric tubes) are long counter-rotating columnar eddies

Turbulent columns with triangular cross sections cannot exhibit rifled rotation in a tube of similar triangular shape, whereas a turbulent flow column in a cylinder can exhibit steady rifled rotation imposed by transverse SH echoing boundary layer sound [10].

Delft scientists, overcame Nikuradse's 1930 technology deficiencies, using computerized transverse tomographic imaging. Coloured particles in water cylinder flow allowed transverse freeze-frame computerized imaging (stereoscopic particle image velocimetry: SPIV). The SPIV transverse slices showed a similar flow pattern in 2, 3, or more equal cylinder sectors, each containing a centripetal radial flow bisecting each sector, flanked by a pair of counter-rotating entrained vortices [11 12]. Fitzgerald idealized the Delft flows, creating an image of a flow pattern that is identical to Nikuradse's transverse flow pattern (figure 6) in a tube with an equilateral cross-section. (One might create more sharply defined SPIV images, similar to the Fitzgerald idealized image, if SPIV particles were selected with the same characteristic acoustic impedance (CIA) as the flowing fluid, so that the particles would not acquire added secondary

deflections from SH boundary layer sound waves [13]. Liebermann's particles displayed epi-cycloidal paths superimposed on their motion away from a SH ultrasound source generating the flow [14].

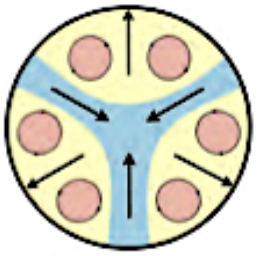

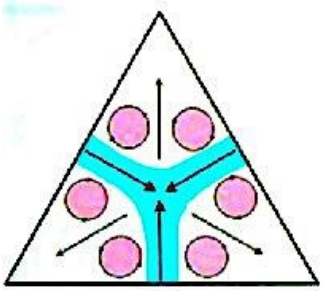

Figure 6: SPIV slice of turbulent flows: Hof; Fitzgerald: 2004 Nikuradse 1930

A central streaming flow, flanked by a pair of counter-rotating vortices is a signature feature of flow away from a simple harmonic (SH) sound [15], or ultrasound [16], generator (figure 7). The flow generator would be the shear forces in the boundary layer, which create oscillations (vibrations) and SH sound waves.

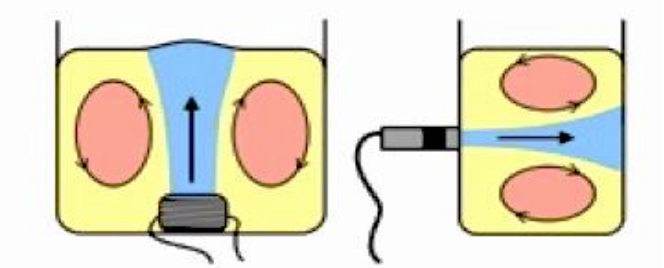

Figure 7: simple harmonic sound generator SH ultrasound transducer

Nikuradse's triangular cross section tubes displayed a centripetal flow band from each mid-wall that entrains two counter-rotating vortices (long counter-rotating straight columnar eddies). If the counter-rotating vortices in cylinders were not involved in the rifling of turbulent flow, they too would be straight counter-rotating columnar eddies. However, the rifled rotation induced by the transverse SH sounds of transition and turbulence, induces the rifling that bends the counter-rotating columns into corkscrew spirals that wind around the mid-axial stream as counter-rotating pairs in identical cylinder sectors. The axially rotating centripetal flow band in a cylinder with a 2-division form would show periodic radial twisting.

In 1929, Dean had found a similar transverse flow pattern in curved cylinders – a single trans-diameter streaming flow from the outer margins of the cylinder's boundary layer to the inside of the curvature, flanked by a single pair of counter-rotating vortices [17]. This distinctive pattern might be explained by the effect of centrifugal force: the curved cylinder's mid-axial stream would be displaced towards the outside of the curvature, causing T-S waves to develop first around the outside curvature where the flow is fastest (the highest rate of shear flow), establishing the trans-diameter flows from the T-S wave origins in the outermost boundary layer. In recent years, the Dean flow pattern [18] attracted the interest of Athanasia Vester at KTH.

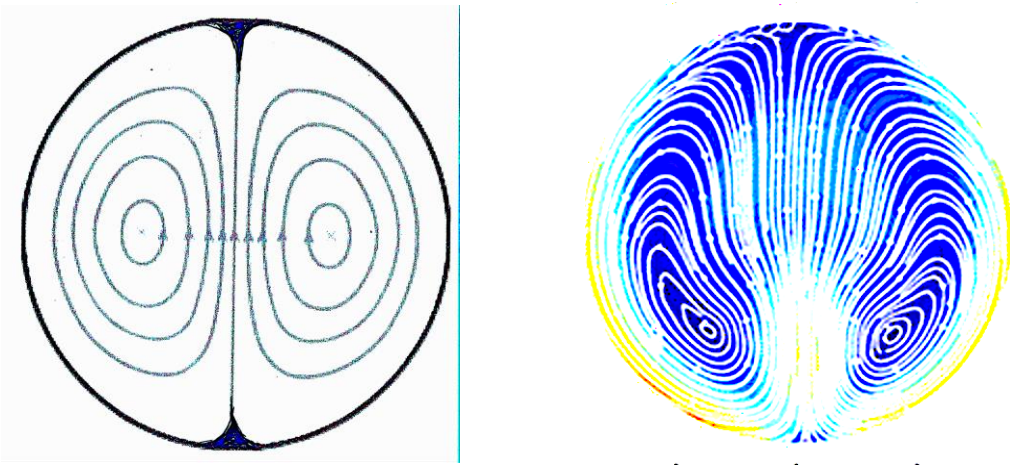

Dean1927 Vester 2015

Figure 8: organized turbulence in curved cylinder

Cylinder flow is unique in that all flow-generated sound is entrapped by sound-reflective walls. Transversely, the entrapped sound reverberates into a resonant SH standing wave frequency corresponding to a natural echoing wavelength of twice the diameter, representing high SH ultrasonic frequencies for most laboratory hydrodynamic cylinder flow studies. The entrapped standing wave sound is focused and propagated longitudinally.

The long straight counter-rotating columns in turbulence in triangular tubes become spiraling corkscrew columns winding around the mid-axial stream in turbulent cylinder flows. When blue colouring is introduced for high pressure and red for low pressure counter-rotating eddies, the appearance resembles a candy cane [19].

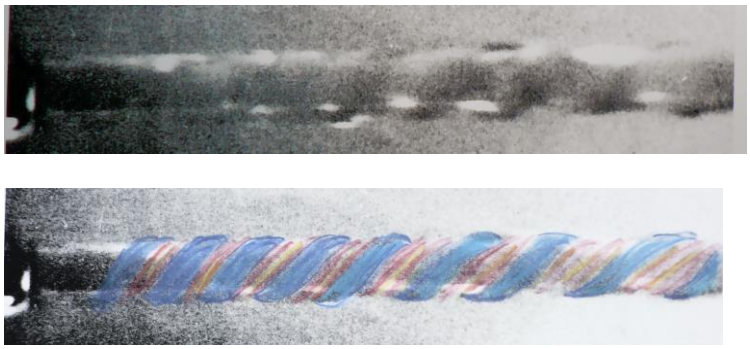

Fig. 9: candy cane high / low pressure bands in rifled efflux turbulent jet

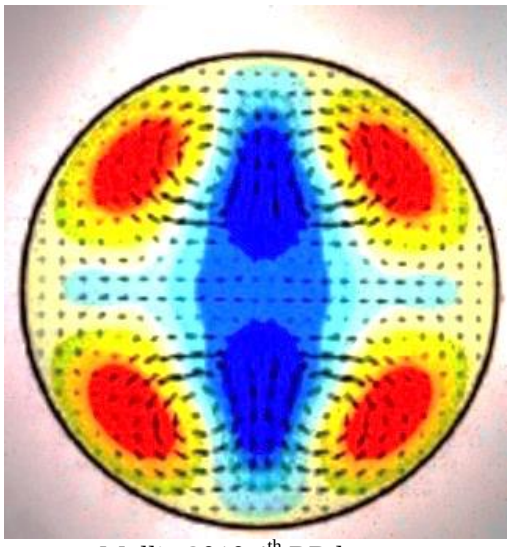

Mullin 2010 4th BB lecture

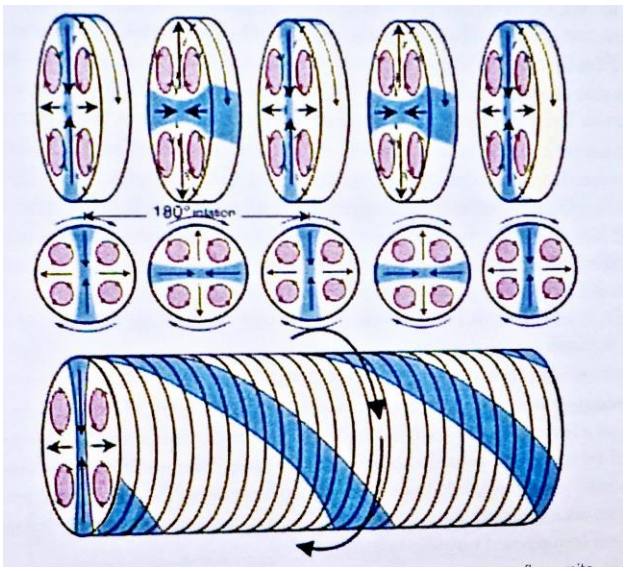

Hamilton 2008: p. 58-61; 2015: p. 7

Fig. 10: 2008 rotating SPIV slices of candy-cane-like turbulent 2-division turbulent column in a cylinder

The transmission of trans-diameter echoing SH sound of late transition, creates high energy oscillating molecules traveling transversely through longitudinally-flowing laminae, transfixing and freezing them, with loss of laminar slip (laminar interlocking), creating a cylinder's flattened iso-velocity profile, with the turbulent water flowing like a non-laminar plug of toothpaste (Prandtl's plug flow [20]). The SH transverse sound waves causing laminar interlocking create the transverse flow patterns through the "frozen" laminae, with distinctive flows in cylinder sector divisions – radial length centripetal bands of flow from the boundary that collide in mid-stream, flanked by a pair of counter-rotating spiral columnar vortices (figures 2, 4, 9 and 10).

A steady axial rotation (rifling) in cylinders, similar to figure 10, was suggested in 1980 [21]: "In cylinders, an axial rotational effect could be permitted, with rotating discoid laminations developing in the plane of the isovelocity profile".

Tyndall's 1867 SH sound splits the efflux jets

Streaming flows in SPIV images, resulting from resonating echoing SH standing wave sound generated in the boundary layer, might explain why Tyndall's sound from a whistle caused turbulence in his laminar water efflux jets from cylinders, simultaneously splitting into 2, 3 or more spinning turbulent jets. Tyndall believed that the SH sound waves of the whistle became superimposed on, harmonized with, and thus amplified, the similar boundary layer SH sound and the transverse flows produced by the sound [22] in 2, 3 or more sectors. These amplified high-pressure centripetal streaming flows, colliding in mid-stream would split the rifled efflux jet into 2, 3, or more spinning efflux jets as the fluid column exits the cylinder [23]. Tyndall did not comment on the spinning, but the rifling was recognized by his illustrator, through the 1/50,000th of a second freeze-frame stroboscopic retinal images produced by periodic electric spark illumination in a dark laboratory [24].

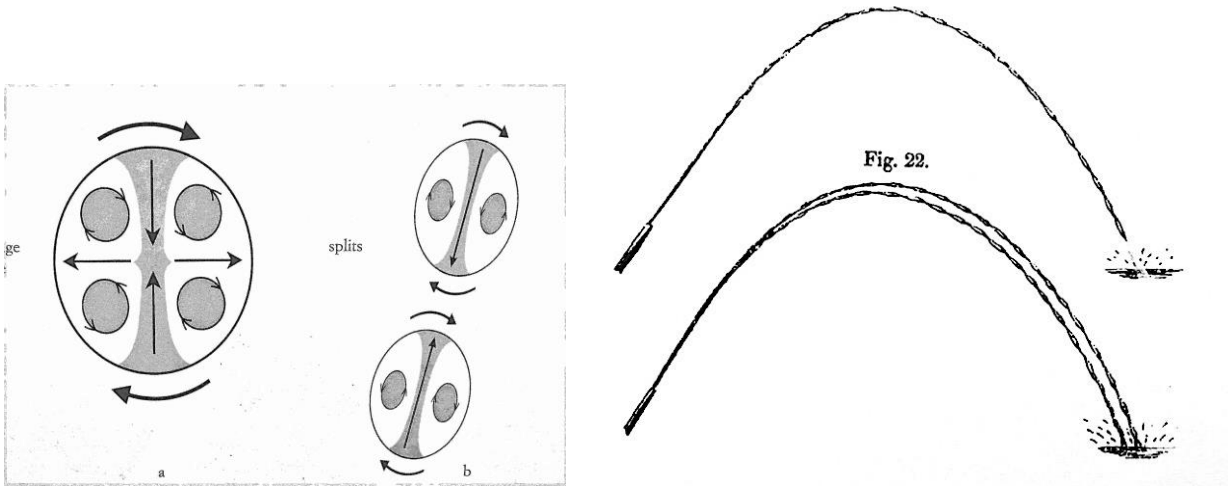

Figure 11: Tyndall's trans-diameter splitting of a cylinder's SPIV 2-division turbulent flow pattern

Tyndall's two types of curling vortices in a dye injection column as turbulence onsets
Figure 12 is from Reynolds 1883 paper, in which he used the stroboscopic effect of periodic spark illumination in a dark room, which created freeze-frame retinal images of 1/2,000th second duration. Reynolds noted that the dye column erupted into "a mass of more or less distinct curls, showing eddies." The adjacent vortices form S-shapes that might represent the counter-rotating eddies found routinely in SPIV transverse tomographic images since 2004 (Hof et al 2004). If this analysis is correct, the axes of rotation of these eddies should be longitudinal, in the plane of the axial flow. The counter-rotating vortices appear when transverse flow-generated sound suddenly creates resonating transverse standing waves, with an echoing wavelength of 2d.

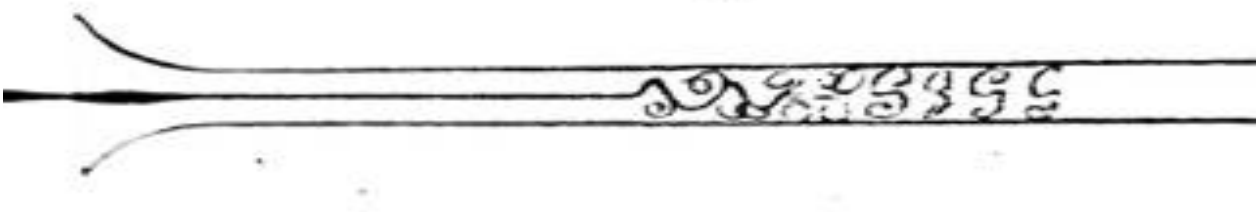

Figure 12: the Reynolds dye injection experiment

On the other hand, the fleeting "flashes of turbulence" Reynolds saw in late transition, now termed "turbulent spots," are pieces of frozen laminae that are ripped out of T-S waves, which roll along in the boundary layer, the axes of rotation being transverse to the flow.

The physics of viscosity-induced flat plate oscillations, vibrations and waves
An oscillation of a mass in a fluid is a vibration that creates a sound wave.

Tollmien [25] and Schlichting [26] theorized that viscosity-induced simple harmonic boundary layer oscillations (T-S shear waves) develop during transition along smooth flat boundaries at

transition flow rates. Contemporary wind tunnels failed to demonstrate the theoretical T-S oscillations.

In the early 1940s, Schubauer and Skramstad took extreme measures in wind tunnel design to eliminate vibrations and noise impinging on the test area (a smooth shiny flat aluminum plate). They discovered SH variations in the velocities of boundary layer laminae, indirectly proving the existence of the predicted SH long-rested boundary layer laminar oscillations in transition. The velocity oscillations gradually increased in amplitude until, just before turbulence, random foci of high amplitude in-phase oscillations appeared, accompanied by noise and vortex formation ("turbulent spots"). Shortly thereafter, as the flow rate continued to rise, many turbulent spots erupted as generalized turbulence prevailed, accompanied by vortices and the aerodynamic noise characteristic of turbulent airflow [27].

A long thin ferromagnetic ribbon, inserted in the boundary layer parallel to the T-S wave fronts, made to vibrate with simple harmonic rhythmicity, would instigate, amplify, or damp the long-crested SH T-S oscillations as particular coherent frequencies were produced by an electromagnet.

Overlooked in discussions of the development of transition's long-crested SH boundary layer shear waves (T-S oscillations), is the obligatory co-generation of SH sound waves. An oscillation of a mass in a fluid is a vibration that creates a sound wave; SH oscillations of a mass of fluid, flowing in the boundary layer as T-S waves, must create SH sound – that is reflected off the boundary transversely into the fluid.

The focally amplified spiking in-phase T-S waves found by Schubauer and Skramstad in late transition were associated with spikes of amplified transverse sound ("noise"), suggesting a cause (sound energy) and effect (vortex formation) relationship in turbulent spots. The sudden appearance of high energy sound waves, propagated from the boundary through the longitudinally sliding laminae, might freeze laminar slip (laminar interlocking) in spots. Abrupt freezing of laminar slip in foci of high amplitude spikes in transverse sound energy might suddenly transfer resistance to the braking effect of the highly resistant boundary, causing head-over-heels vortices (turbulent spots) to be ripped out of the fast-flowing long-crested wave fronts. The turbulent spot vortices roll downstream with the flow. The sudden emergence of many random turbulent spots, with many vortices and high flow resistance, signifies generalized laminar interlocking of turbulence, accompanied by aerodynamic noise.

One can understand how a transverse linear boundary imperfection (e.g., a knife edge) might force all nascent turbulent spots to emerge together along a T-S wave front in late transition, creating the simple harmonic sound in standing wave form, known as edge tones [28 29]. Furthermore, a similar transverse boundary impediment in a shallow turbulent stream may cause turbulent spot vortices to re-align and re-form the SH long-crested T-S waves out of which they were ripped as turbulence onset; thus, an area of SH long-crested stationary waves might occur within a stream flow that elsewhere displays turbulent waves (similar to figure 12).

T-S waves are composed of two SH waveforms. BLF (boundary layer flutter) waves represent the primary dynamic grabbing-and-releasing viscosity-induced shear waves, which strike simultaneously towards the boundary in the grabbing phase and then rebound upwards – the source of the vibrations that create SH transverse sound. The LM (laminar membrane) waves represent the SH long-crested wavy paths along which the BLF waves travel. The wavy paths

slide along the shiny flat plate boundary at a velocity much less than the average flow velocity, unless arrested by a linear transverse boundary imperfection (Fig. 11), which reveals the unsuspected standing wave nature of LM waves.

Benjamin, studying laminar flows over a stationary rigid boundary made up of long-crested SH waves (a corrugated galvanized steel panel), intuitively introduced the concept of SH standing waves in shear flows. If the panel were placed on another long flat smooth panel lubricated with oil, the water's viscosity would "entrain" the panel, making it slide in the direction of flow at a velocity lower than the average fluid velocity. The panel would duplicate the actions of LM waves, the paths along which laminae flutter (as boundary layer flutter, BLF, waves) during transition. Just as a transverse linear deformity on the oiled boundary arrests the panel, in water flow in a shallow stream, a linear transverse impediment on the boundary (the limestone stream bed) arrests LM waves, revealing their standing wave nature (figure 13) [30].

Figure 13: Transverse boundary imperfection in a limestone stream bed arrests SH LM waves

Schubauer and Skramstad found the predicted long-crested SH viscosity-induced boundary layer T-S oscillations. However, T-S waves are composed of two inter-related forms of shear waves:

1) boundary layer flutter (BLF) waves in each adjacent lamina (all similar in form, with velocities increasing as the distance from the boundary increases)
2) the simple harmonic wavy paths that have the same form as the BLF waves, but which move at a velocity much slower than the average velocity of the BL waves that make up the flow.

At sub-transitional flow rates, each boundary layer lamina is planar, acquiring a momentum-based directional stability, acting like a membrane under tension. As the velocity increases, the momentum-related tension increases (like tightening the diaphragm of a drum). In late transition, the viscosity-induced grabbing-and-releasing along the boundary creates long-crested SH oscillations (laminar membrane, or LM waves); LM waves are composed of the identical paths along which each SH BLF lamina flows, regardless of the varying laminar velocities.

The dichotomy of SH velocity oscillations and BLF waves

During transition in water flow, BLF waves flow up and down along paths (LM waves) that slide along much more slowly than the average rate of flow. Any divergence of one liquid lamina from its neighbours would result in cavitation. The laminae cannot converge on each other (as shown in figure 13) because liquids are incompressible. Thus, in liquid laminar flow, each lamina must conform exactly to its abutting neighbours [31]. Since transition to turbulence in air flow duplicates water flow, air laminar shear waves (BLF waves) must also conform to each other.

Using hot wire anemometers at periodic distances from in the boundary layer, Schubauer and Skramstad, identified SH variations in laminar velocities as the distance from the boundary increased. Thus, they proved, indirectly, the existence of SH physical fluid waves in the laminae, but velocity oscillations are only graphical representations of velocity (Fig. 14), not physical shear waves. They believed that the fluid waves would duplicate the velocity oscillations [32].

The difference between velocity oscillations and the physical fluid wave motion can be imagined by considering a block of fluid one lamina in thickness on the boundary (figure 15). During the first appearance of a shear wave, as the anterior superior corner of the block arches forwards and downwards towards the boundary (grabbing phase) it increases in forward velocity. At the same time, the anterior inferior corner of the block arches downwards and backwards, decreasing the forward velocity, 180 degrees out of phase. Simultaneously, a series of equidistant points on the posterior of the block would describe identical (in phase) SH wavy paths, duplicating the physical motion of the fluid shear waves.

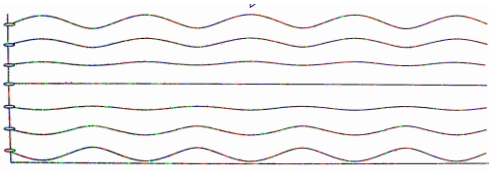

Figure 14: Velocity oscillations reverse phase as distance from boundary increases

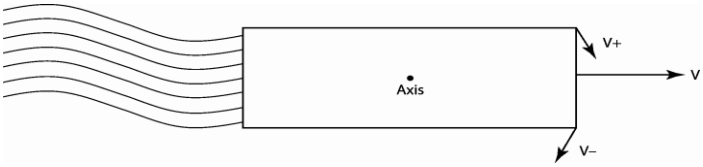

Figure 15: Physical fluid waves remain in phase as distance from boundary increases

The overlooked SH waves on the boundary under LM (and BLF) wave crests

Under the crests of water LM waves on a flat plate boundary (figure 16), there must be sub-LM waves (which may also be termed sub-BLF waves) or cavitation would occur. Because of viscosity and the friction of the boundary, sub-LM water is entrapped, entrained as long columnar eddies, which roll along the boundary at the velocity of the LM waves. When water (a compliant laminar fluid) is the boundary and wind, the fluid flowing along it, the long columnar sub-LM eddies roll over and crash on the shore (“rollers” or “breakers”), as the bottoms of the rotating columns are slowed by sea floor contact in the shallows.

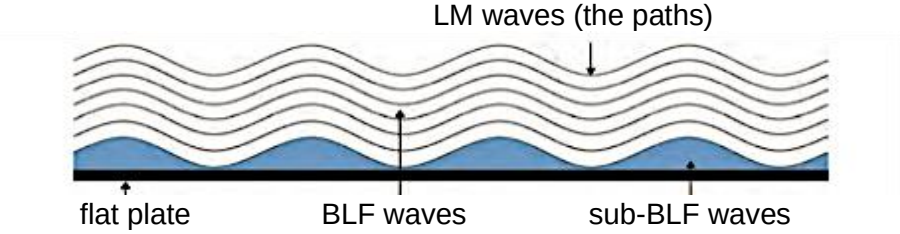

Figure.16: BLF, LM and sub-BLF waves (Hamilton 2011)

The preceding discussion suggests that the phenomenon of turbulent flow results from transverse simple harmonic sound, co-generated with the T-S oscillations of transition, which induces laminar freezing (laminar interlocking), transferring friction abruptly to the high

resistance of the boundary, creating many turbulent spots with noise. In cylinders, the sounds of transition and turbulence reverberate, echoing back and forth, producing resonant sound with a natural SH frequency (corresponding to a wavelength of 2d), which is specific for each cylinder's internal diameter. 8,000 vps is the upper limit of audible frequencies for most males, equating to an internal cylinder diameter (water flow) of about 9.4 cm. Thus, all laboratory fluid flow experiments using cylinders of less than 9.4 cm would generate inaudible echoing SH transverse ultrasound – explaining why SH sound generation in cylinders has been generally overlooked.

Since sound is propagated in all directions, there would be similar standing wave sound focused along the cylinder, with a wavelength of twice the diameter, accounting for Thomas's glass bead waves accumulating at 1/2 wavelength intervals during transition and in turbulence [33]. The glass bead waves slide slowly along the shiny glass tube, entrained by viscosity (like a Benjamin corrugated steel SH wavy boundary sliding along an oiled flat boundary, as discussed previously).

The enigma of arteriographic standing waves (figure 17) can be explained similarly. The periodic high / low pressure bands of standing wave sound produce the circumferential waves that indent the compliant arterial wall. Since arterial diameters are usually less than 1 cm., the resonant sound creating the SH pressure bands is above 100,000 vps. (There has been a tendency over the years to consider that the wavelength of such an arteriographic standing wave is the diameter [34]; however, the wavelength of a standing wave is twice the distance from loop to loop, or node to node, which equates to 2d for echoing transverse sound in cylinders).

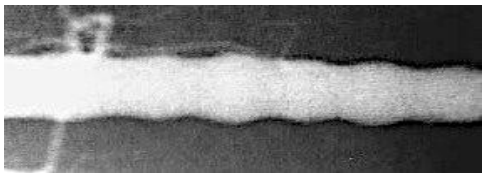

Figure 17: Arteriographic standing waves

This accounts for Thomas's [35] finding that, in transition and in turbulent water flow in cylinders, tiny glass beads accumulate at 1/2 wavelength intervals in glass cylinders. These slide along the shiny tube by viscosity entrainment [36]. Similarly, Bagnold showed photographically that at turbulent flow rates (wind or water) sand particles were ejected at right angles from the troughs of SH sand waves and deposited at shallow angles on the crests in transition and in turbulence, consistent with the physics of the Kundt's tube standing wave sound experiment. Thomas believed that the glass bead waves and Bagnold's sand waves shared the same physics. Entrained glass bead waves in standing wave form can slide along on smooth shiny glass cylinders, but sand waves cannot slide on sand.

Compliant boundary (CB) waves

Essapian's photographs of speeding dolphins showed SH circumferential skin waves (fig. 18), which were aligned with the dermal ridges, appearing along the epidermis (a compliant boundary); he believed the CB waves were related to the dolphin's hydrodynamic advantage [37], preserving laminar flow resistance. Transverse boundary imperfections (ridges) might arrest LM waves, revealing the stationary periodicity of pressure bands associated with SH stationary LM waves (as in figure 13).

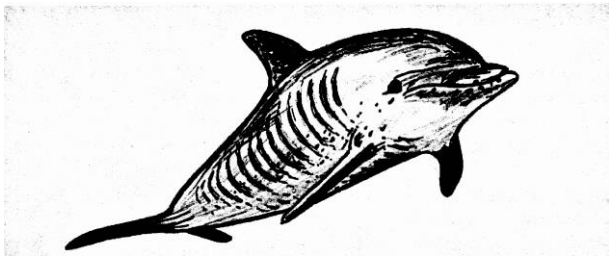

Figure 18: Essapian's speed-induced (LM) standing waves on dolphin skin

A stretch of flat sand represents a compliant particulate boundary that damps turbulent spot formation, retaining the SH long-crested form of transition's T-S waves, and revealing a standing wave nature. These SH long-crested sand waves, in the face of turbulent wind flow rates, caused Bagnold to ponder: " ....instead of finding chaos and disorder, the observer never fails to be amazed at a simplicity of form, an exactitude of repetition and a geometric order." (R.A. Bagnold 1941).

Interfaces between two fluid layers involved in shear interaction represent other examples of compliant boundaries. Fluid interfaces display the high / low SH pressure bands created by the grabbing / releasing viscosity interaction. SH waves on water in the wind demonstrate a gas / liquid shear interface. SH clouds seen commonly in a windswept sky reveal CB long-crested shear waves between air strata of different temperature and moisture content.

Figure 18: lingering contrail of a jet aircraft in a clear sky reveals SH interstratum CB shear waves

The Reynolds U-tube experiment reveals SH shear waves along an interface (boundary) between two liquids of different specific gravity. Similarly, one can understand how isolated high amplitude sea waves can occur if the wave crests of underwater shearing currents close to the water surface are superimposed on wave crests of wind-induced waves, creating the large "rogue waves" that have menaced mariners since man first sailed the seas.

Damping the BLF waves and the SH sound they produce

The dynamic BLF waves are the primary shear waves of transition, creating the transverse boundary layer sound responsible for the laminar interlocking that causes the high flow resistance and vortices of turbulence. Damping (actively, or passively) the BLF waves and / or

the transverse sound they produce should preserve laminar flow with its lower resistance. The compliant tissue of our fingertips can damp the vibrations of a ringing bell. Similarly, a dolphin's compliant skin should damp, passively, the SH BLF waves and the sound they produce [38]. Kramer achieved "distributed damping" by using rubber layers separated by a type of silicone that he selected (intuitively) because of its ability to damp standing wave sound. Kramer's coverings on underwater projectiles delayed the onset of turbulence [39 40].

The transverse surface bands (ridges) in dolphins' compliant skin and the surface bumps (denticles) of shark skin may interfere with BLF wave development, preventing the amplification that triggers turbulence, and may exhibit the same effect of lowering resistance as the dimpling of a golf ball surface. In addition, the large, highly developed temporal lobes of a dolphin's brain, an area dedicated to auditory processing circuitry, might be using feedback from skin vibration (sound) sensors to stimulate skin muscle contractions to damp, actively, the SH BLF waves and the sound they produce (olivo-cerebellar spatiotemporal phase reset mechanisms [41]).

If subcutaneous blood vessels are similarly controlled by olivo-cerebellar-temporal feedback from skin sensors, blood vessels might be constricted along transverse bands aligned with the dermal ridges. Body fat is solid at room or seawater temperatures. Skin vessel constriction could lower subcutaneous fat temperature through seawater contact, causing the fat to become more solid in SH bands that might damp the dynamic BLF waves [42].

Similarly, one might use surface vibration / pressure sensors along a compliant boundary (e.g. – Teflon) with narrow transverse compartments (like Carpenter's transverse damped panels), filled with rheo-magnetic fluid, to damp developing BLF waves by negative feedback to the conductive rheo-magnetic fluid. The developing waves might be damped by electronically computerized alteration of the stiffness of the boundary in bands corresponding to the long-crested SH BLF waves of transition [43] (Essapian's circumferential CB standing waves).

Bird's feathers damp, passively, the SH sound created by BLF waves. Furthermore, fanned out wing tip feathers of soaring eagles may have active muscle feedback control similar to Carpenter's damped rigid panels, which are known to delay turbulence to very high Reynolds numbers [44]. Each feather is composed of large numbers of compliant micro-panels that must cause some sound deadening and might be involved in damping BLF waves as well [45].

Conclusion

What have been considered as T-S waves integrate three different SH wave forms

1. BLF (boundary layer flutter) waves – the dynamic primary waves
2. LM (laminar membrane) waves – the paths that BLF waves flutter along at individual laminar velocities; LM waves have velocities much less than the average flow velocity – and may be stationary, revealing a standing wave nature.
3. Sub-BLF (also may be termed sub-LM) SH rolling columnar waves on the boundary, under the LM (and the BLF) wave crests. Sub-BLM waves move at the speed of LM waves

When the boundary is compliant, the sub-BLF waves are replaced by SH compliant boundary (CB) waves.

Damping the dynamic BLF waves and / or the transverse sound they produce, should preserve laminar flow by delaying the onset of the high resistance laminar interlocking, the cause of turbulent flow.

The analysis of the physics of T-S wave development is a significant component of this theory to explain the mystery of transition to turbulence. After centuries of study, there is no competing theory.

---

[1] Schlichting H: Boundary-Layer Theory (Sixth edition, 1968), McGraw-Hill, New York.
[2] Hair DS, Fresh Strange Music – Elizabeth Barrett Browning's Language, McGill-Queens University Press, London, Ontario, 214-217, 2015
[3] Browning EB, 1858, Aurora Leigh, Chapman and Hall, Book 8, lines 44 – 48 (1857)
[4] Leconte J: On the influence of musical sounds on the flame of a jet of coal gas. Phil Mag (1859); 15: pp. 235-239
[5] Tyndall J: On the action of sonorous vibrations on gaseous and liquid jets. Philosophical Magazine (1867); 33: pp. 375-391.
[6] Hamilton G, Patterns in Fluid Flow Paradoxes – Variations on a Theme. UWO Graphic Services, London, Ontario, 1980: 59-62
[7] ibid: p. 59: p. 70
[8] Hof B., Van Doorne, C.W.H., Westerweeel J., Nieustadt F.T.M., Faisst H., Eckhardt B., Kerswell R.R., Waleffe F., Experimental observation during slow flow of non-linear traveling waves in turbulent pipe low. Science; 305: 1594-1598 (2004)
[9] Mullin T, Darbyshire AG, Hof B, Juel A, Peixhino J, Tasaka Y, The Enigma of The Transition to Turbulence in a Pipe. 4th Brooke Benjamin Lecture (2010)
[10] Hamilton G, Simple Harmonics. Aylmer Express, Aylmer, Ontario; 2015: 33-35
[11] Hof 2004
[12] Fitzgerald R. New Experiments set the scale for the onset of turbulence in pipe flow. Physics Today: pp. 1-5 (February 2004)
[13] Hamilton G, Transition to Turbulence – Dynamic Standing Waves. UWO Graphic Services (2009): 26
[14] Liebermann LN: The second viscosity of liquids. Physical Review. (1949)
[15] Gaines N: A magnetostriction oscillator producing intense audible sound and some effects obtained. Physics (1932); 3: pp. 209-229.
[16] Liebermann LN (1949)
[17] Dean WR, Note on the Motion of Fluid in a Curved Pipe, Phil. Mag. J. Sci. 4:208-223, 1927
[18] Vester, AK, Örlü R, and Alfredsson PH, Turbulent Flows in Curved Pipes: Recent Advances in Experiments and Simulations. Appl. Mech. Rev 68(5), 2016
[19] Hamilton G, (2008): 58-62
[20] Prandtl L and Tietjens OG: Applied hydro- and Aeromechanics. Dover Publications, New York (1957) (reprint of 1934 edition): p 30-36
[21] Hamilton 1980: 63
[22] Tyndall J, 1867
[23] Hamilton G, The Physics of the Sound Barrier, Brownian Motion and Tyndall's Sonorous vibrations (2012 Supplement to Order in Chaos). Aylmer Express Aylmer Ontario; 2012; pp 8-10
[24] Hamilton G, (2008): 50
[25] Tollmien W. Über die Enstehung der Turbulenz. 1. Mitteilung, Nachrichten der Gesellschaft der Wissenshaften zu Göttingen, Mathematisch – Physikalische Klasse, Report I, Göttingen Scientific Society, 21-44 (1929)
[26] Schlichting H., Über die Enstehung der Turbulenz bei der Plattenströmung; from Nachrichten der Gesellschaft der Wissenschaften zu Göttingen, Mathematisch-Physikalische Klasse, 181- 208 (1933)

[27] Schubauer G.B. and Skramstad H.K., Laminar-boundary-layer-oscillations and transition on a flat plate. Advance Confidential Report. National Advisory Committee to Aeronautics, 1-70 (1943)
[28] Krüger F: Theorie der Schneidentöne. Annalen der Physik (1920); 62: pp. 672-690
[29] Hamilton 2015: 16
[30] Hamilton, Order in Chaos – The Physics of Transition to Turbulence. Aylmer Express, Aylmer, Ontario; 2011: 57
[31] ibid
[32] Hamilton G., Order in Chaos – The physics of transition to turbulence. Aylmer Express (2011)
[33] Thomas DG: Periodic phenomena observed with spherical particles in horizontal pipes. Science (1964); 144: pp. 534-536
[34] New PFJ: Arterial Stationary Waves. AJR (1966); 97: pp. 488-499
[35] Thomas DG: 1964
[36] Hamilton G., Simple Harmonics, Aylmer Express, 2015, p. 10
[37] Essapian, F.S. Speed-induced skin folds in the bottle-nosed porpoise, Tursiops truncatus. Brev., Mus. Comp. Zool. 43, 1-4. (1955).
[38] Gray, J. Studies in animal locomotion. VI: The propulsive powers of the dolphin. J. Exp. Bio., 13, 192 -199 (1936)
[39] Kramer MO. Boundary layer stabilization by distributed damping. American Society of Naval Engineers Journal (1960); 72: pp 25-33.
[40] Hamilton 1980, 2015: p.15
[41] Bandyopadhyay, P.R. & Hellum, A.M. Modeling how shark and dolphin skin patterns control transitional wall-turbulence vorticity patterns using spatiotemporal phase reset mechanisms. *Scientific Reports*, 4, Article number: 6650 (2014).
[42] Hamilton 2015: p.15
[43] ibid
[44] Carpenter, P.W., Davies, C. and Lucey, A.D. Hydrodynamics and compliant walls: does the dolphin have a secret? Curr. Sci., 6: 758-764 (2000)
[45] Hamilton 1980; 2015: p.15